第 25 卷第 4 期 无 机 化 学 学 报 Vol.25 No.4
2009 年 4 月 CHINESE JOURNAL OF INORGANIC CHEMISTRY 635~640

SiO_2:Sm 粉体:溶胶-凝胶法制备及特殊荧光性能

谭伟民 陆春华* 倪亚茹 王晓钧 许仲梓
(南京工业大学材料化学工程国家重点实验室,南京 210009)

摘要: 采用溶胶-凝胶法制备 SiO_2:Sm 粉体,通过 TG-DSC、FTIR、MAS-NMR、PL 对材料的结构和性能进行测试表征。FTIR 分析显示样品位于 960 cm^{-1} 的吸收峰归属于 Si-O-Sm 键的变形振动,^{29}Si MAS-NMR 证实 Sm^{3+}进入 SiO_2 网络结构。在 380 nm 入射光激发下样品产生除 Sm^{3+}特征发光以外的蓝绿荧光,对不同 Sm^{3+}掺量样品荧光性能进行对比分析,结果表明这种特殊的荧光发射与 Si-O-Sm 键的形成有关。

关键词: SiO_2:Sm; 溶胶-凝胶; 光致发光; Si-O-Sm 键
中图分类号: O613.72; O614.33+7; TQ133.3 **文献标识号**: A **文章编号**: 1001-4861(2009)04-0635-06

Unique Photoluminescence in SiO_2:Sm Prepared by Sol-Gel Process

TAN Wei-Min LU Chun-Hua* NI Ya-Ru WANG Xiao-Jun XU Zhong-Zi
(*The State Key Laboratory of Materials-Oriented Chemical Engineering, Nanjing University of Technology, Nanjing* 210009)

Abstract: SiO_2:Sm powders prepared by the sol-gel process were structurally characterized by thermogravimetric-differential scanning calorimetry (TG-DSC), Fourier transform infrared (FTIR) spectraoscopy and ^{29}Si magic angle spinning nuclear magnetic resonance (MAS-NMR). The peaks near 960 cm^{-1} in FTIR results are assigned to the deformation vibration of Si-O-Sm linkages, and the samarium ion has been incorporated into the framework of SiO_2 as validated by ^{29}Si MAS-NMR. Blue-green and red photoluminescence (PL) emission in structural disordered SiO_2:Sm powders was observed at room temperature with excitation at 380 nm. Study on the luminescence spectra of SiO_2:Sm powders with different doping concentrations of Sm^{3+} indicates that the generation of the special PL band is related to the formation of Si-O-Sm linkages.

Key words: SiO_2:Sm; sol-gel; photoluminescence; Si-O-Sm linkages

Lanthanide complexes are attractive materials for optical applications like display and illumination owing to their excellent luminescence catalytic, electric and magnetic properties, which are attributed to the electronic transitions between the 4*f* energy levels[1~5]. However, sometimes these applications are limited due to their poor thermal stabilities and low mechanical strength[6,7]. These drawbacks can be overcome by incorporating these complexes into solid matrices. Many lanthanide complexes have been incorporated into silica either by simple doping method (no strong bonding between the phases) or by covalent bond grafting technique using low-temperature soft-chemistry processes to circumvent these shortcomings[8~13] such as sol-gel derived hybrid materials. Compared to the pure lanthanide complexes, the obtained hybrid materials show stronger luminescent intensities and higher quantum efficiencies[12~15]. As an example, Eu-MCM-41 system was prepared by incipient wetness method. The Eu-MCM-41seems to be a promising luminescent

收稿日期:2008-11-03。收修改稿日期:2009-02-18。
江苏省自然科学基金项目(No.BK2004121),教育部跨世纪优秀人才项目,江苏省高校自然科学基础研究项目(No.08KJB480001)资助。
*通讯联系人。E-mail:chhlu@njut.edu.cn, atan0910@163.com
第一作者:谭伟民,男,26 岁,博士;研究方向:光学功能材料。

material for high resolution devices and technologies of selective optical sensors[16].

In the other way, more attention has been focused on visible photoluminescence at room temperature in disordered materials these years because of their potential technological applications on the development of new luminescent materials such as flat-screen full-color displays and compact laser devices operating in the blue region to develop new generation of DVD record[17,18]. The high PL emission requires some degree of structural order together with a certain amount of structural disorder in these materials. Blue-green and red photoluminescence has been detected due to the interaction of TiO_5-TiO_6 in $CaTiO_3$:Sm[19]. Blue-light PL emission at room temperature has also been observed in $SrTiO_3$(STO) ascribed to the oxygen deficiency[20]. It can be concluded that a more intense PL emission is obtained for a certain order-disordered structure.

In this work, a blue-green and red luminescence of SiO_2:Sm compound is reported. Rare earth ions (Sm^{3+}) are used to substitute Si^{4+} and incorporate into the Si-O framework. FTIR spectroscopy and ^{29}Si MAS-NMR are used to characterize the introduction of samarium ions into the Si-O framework. The results are structural characters for a better understanding of the PL emission processes in terms of the local structure around silicon atoms.

1 Experimental

1.1 Synthesis

Samarium nitrate was obtained by dissolving Sm_2O_3(99.9%) in concentrated nitric acid. All the other reagents were analytical pure. A typical procedure for the preparation of SiO_2:Sm powders doped with different concentrations of samarium ions is illustrated in Fig.1. Firstly, precursor solution was prepared by magnetic stirring tetraethoxysilane (TEOS), H_2O, and ethanol (TEOS:H_2O:ethanol=1:10:4) at room temperature for 30 min. The pH value was adjusted to ca. 2~3 by dripping 1 mol·L^{-1} nitric acid. Secondly, $Sm(NO_3)_3$ and organic additives were added into the precursor solution to get different doping concentrations of Sm^{3+} from 2.5mol% to 20mol% with the pH value being controlled at ca. 2~3, and the ultimate solution was dispersed by ultrasonic at 60 ℃ for 30 min. Finally, xeorgel was thermal treated at 700 ℃ for one hour to get SiO_2:Sm powders.

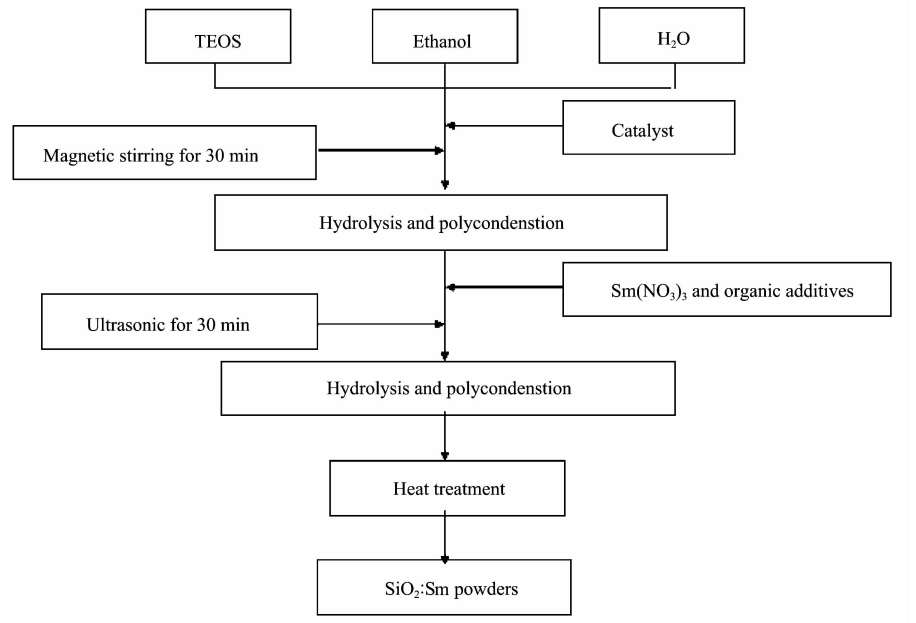

Fig.1 Sol-gel preparation scheme for SiO_2:Sm powders

1.2 Characterization

In order to get appropriate temperature of thermal treatment the TG-DSC analyses were performed on STA449C synthetical thermo-analysis instrument from

the thermal balance at 20 to 760 ℃ with a temperature ramp of 10 ℃·min^{-1} in static air atmosphere. Infrared spectra were recorded in 4 000~400 cm^{-1} region by FTIR-360 Fourier transform infrared spectrometry from Nicolet, USA. SiO_2:Sm powders were tested by ^{29}Si MAS-NMR. The NMR measurements were conducted at 300 K with a frequency of 79.49 MHz on a Bruker AV-400D spectrometer using acetone as solvent. The reference material for the chemical shift was tetramethylsilane(TMS). The photoluminescence spectra were measured at room temperature with a spectrophotometer(Jobin Yvon Fluorolog3-221) using a Xe lamp(450 W) as excitation source, and focused by off-axis mirror for maximum efficiency at all wav elengths.

2 Results and discussion

2.1 TG-DSC

There are two stages of weight loss in the TG curve, as shown in Fig.2. Firstly, from room temperature to 240 ℃, 33.04% weight loss is due to the evaporation of the water and solvent, and Si-OH aggregation of SiO_2 microstructure. Secondly, from 240 to 750 ℃, about 20.28% weight loss is due to the evaporation of the remnant solvent and the pyrolysis of organic compounds. DSC thermogram of SiO_2:Sm xerogel shows a strong endothermic peak around 136.4 ℃, which is assigned to the evaporation of absorbed water and ethanol in the holes of the gel and aggregation of Si-OH. The exothermic peak at 599.3 ℃ can be attributed to the decomposition of organic additives. The thermal temperature in this experiment was set at 700 ℃ based on TG-DSC results.

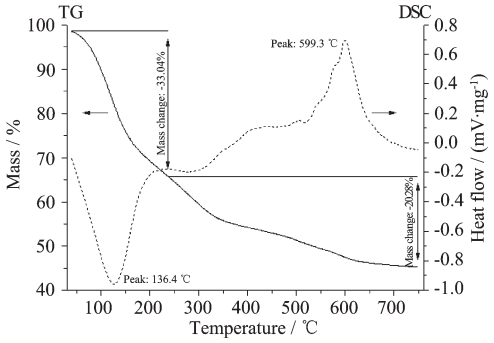

Fig.2 TG-DSC curves of SiO_2:Sm xerogel

2.2 FTIR spectra

The FTIR spectra of SiO_2:Sm xerogels with different doping concentrations of Sm^{3+} are shown in Fig.3. The broad bands around 3 450 cm^{-1} may be attributed to the surface silanols and adsorbed water molecules, while the deformational vibration of -OH causes the absorption bands at 1 650 cm^{-1}. The bands at 950 cm^{-1} and 571 cm^{-1} correspond to the stretching and bending vibrations of the Si-OH groups[21,22]. The strongest absorption bands relative to the silica structure, appearing in the range between 1 000 and 1 300 cm^{-1}, are due to the Si-O-Si groups asymmetric stretching vibration mode, whereas the peaks near 800 and 446 cm^{-1} originate from the symmetric stretching and bending vibrations of the Si-O-Si groups, respectively[23]. It can be seen that absorption bands around 1 064 cm^{-1} are splited with the increasing samarium content, which are ascribed to the Si-O-Si groups asymmetric stretching vibration mode. At the same time, the Si-O-Si groups symmetric stretching mode near 800 cm^{-1} also blue shifts from 792 to 815 cm^{-1} when the doping concentration of Sm^{3+} is increased. These phenomena illuminate that the doping of Sm^{3+} has

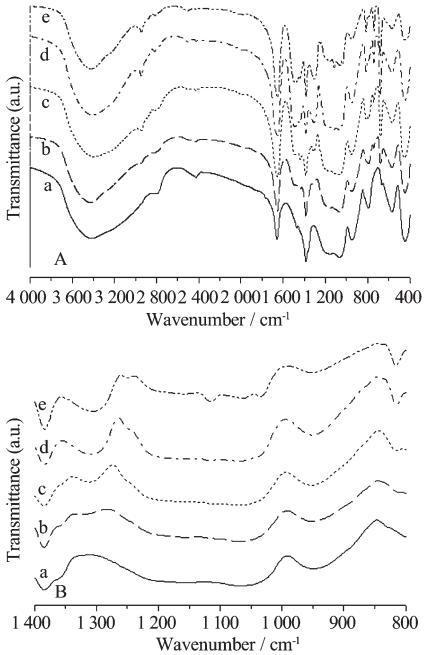

(a) SiO_2; (b) 2.5 mol%; (c) 5 mol%; (d) 10 mol%; (e) 15mol% (B is a part enlarged area of A)

Fig.3 FTIR spectra of SiO_2:Sm xerogels with different doping concentrations of Sm^{3+}

influenced the [SiO_4] framework. Maybe it is due to the introduction of samarium ions into the framework and Si-O-Sm linkages formation.

Fig.4 shows the FTIR spectra of samples with different doping concentrations of Sm^{3+} thermal treated at 700 ℃. The O-H stretching and O-H bending vibration modes located at 3 450 cm^{-1} and 1 650 cm^{-1} are still evident in the FTIR spectra. The vibrations of the Si-OH groups at 950 cm^{-1} and 571 cm^{-1} are disappeared after thermal treatment. Its the evidence that high temperature urges the combine of Si-OH. It can be found that the Si-O-Si groups asymmetric stretching vibration mode near 1 100 cm^{-1} red shifts from 1 103 to 1 070 cm^{-1} with the increasing doping concentrations of Sm^{3+}. Furthermore, spectra changes near 960 cm^{-1} are observed by increasing samarium content. The new vibration peak located at 960 cm^{-1} is assigned to the metals incorporation into the framework of silica materials[21,24,25]. These effectively substantiate the formation of Si-O-Sm linkages.

2.3 ^{29}Si MAS-NMR

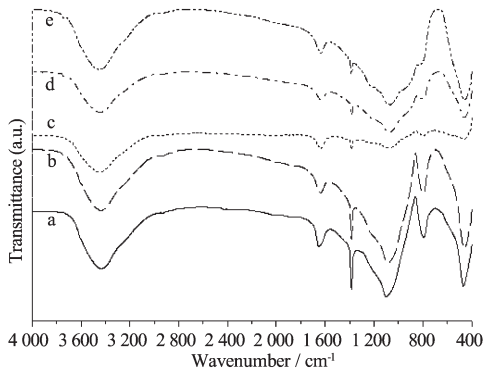

(a) SiO_2; (b) 2.5mol%; (c) 5mol%; (d) 10mol%; (e) 15mol%

Fig.4 FTIR spectra of samples thermal treated at 700 ℃ with different doping concentrations of Sm^{3+}

The ^{29}Si MAS-NMR spectra of xerogels, reported in Fig.5, are due to the convolution of three peaks. The first peak, Q^2, centers at around −84 ppm, is due to the contribution of silicon atoms bearing two hydroxyl groups $(Si\text{-}O)_2\text{-}Si\text{-}(OH)_2$ (geminal silanols), the second peak, Q^3, at around −94 ppm, is due to the silicon atoms bearing one hydroxyl group and the third peak, Q^4, at around −104 ppm, is due to the silicon atoms without hydroxyl groups[26,27].

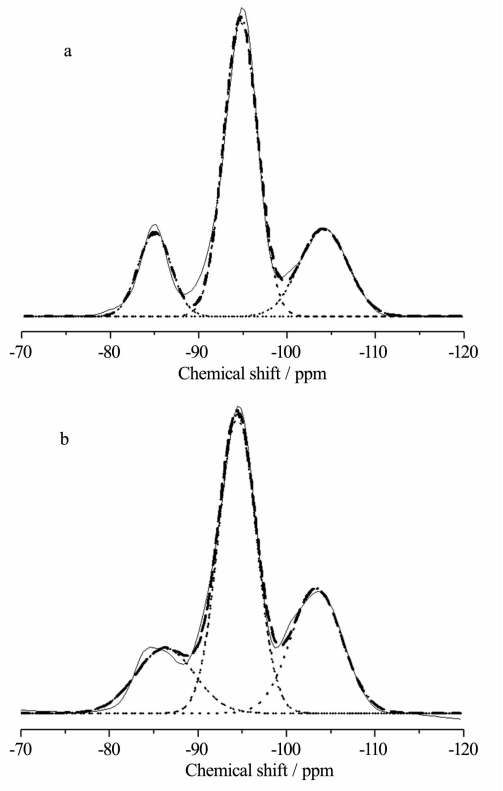

(a) SiO_2; (b) $n_{Sm^{3+}}/n_{SiO_2}$=15%. Peaks deconvolution (fit results: dashed line; single Gaussian: dotted lines)

Fig.5 ^{29}Si-MAS NMR spectra of xerogels

Assuming that Q^2, Q^3 and Q^4 chemical shift positions do not change, a comparison between the relative contribution of the three different silicon atoms is possible. To evaluate the area of the three peaks deconvolution has been performed by means of three Gaussians keeping fixed the chemical shifts values to −84, −94, −104 ppm and varying the full-width-at-half-maximum (FWHM) plus with the peak intensity. Significant changes are observed by increasing doping samarium content, as shown in Table 1. It is worth noting that Q^2 area does not change significantly, while Q^4 and Q^3 area increases and decreases, respectively. It is probably due to the conversion of $(Si\text{-}O)_3\text{-}Si\text{-}OH$ groups to $(Si\text{-}O)_3\text{-}Si\text{-}O\text{-}Sm$ groups according to the shift

Table 1 Peak areas obtained by deconvolution of the ^{29}Si MAS-NMR spectra(a) SiO_2, (b) $n_{Sm^{3+}}/n_{SiO_2}$=15%

Samples	Q^2 / %	Q^3 / %	Q^4 / %
a	16.15	59.11	24.74
b	17.77	52.45	29.78

of Si-O-Si groups stretching mode in FTIR spectra analysis.

Fig.6 shows ^{29}Si MAS-NMR spectra of samples thermal treated at 700 ℃. It can be seen that the SiO_2 sample has no visible peaks. The small peak near −100 ppm is attributed to sympathetic vibration. Thus, the structure of this sample may be incompact layer frame, as shown in Fig.7a. However, there is a strong peak at −109 ppm relative to SiO_2:Sm sample with 15mol% doping concentration of Sm^{3+}. The reason could be attributed to the fact that samarium ions incorporation into the Si-O framework attracts the electron cloud of oxygen, and it is beneficial for the formation of Si-O framework. Fig.7b shows the framework of SiO_2:Sm.

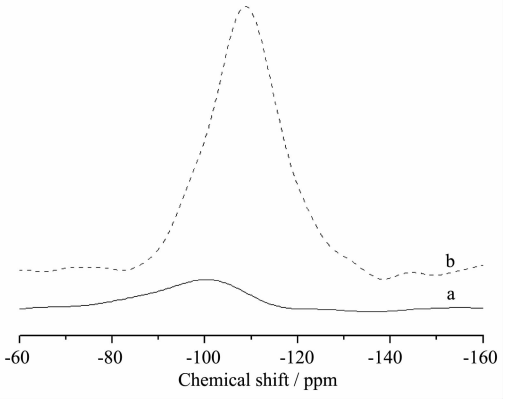

(a) SiO_2; (b) $n_{Sm^{3+}}/n_{SiO_2}$=15%

Fig.6 ^{29}Si-MAS NMR spectra of samples thermal treated at 700 ℃

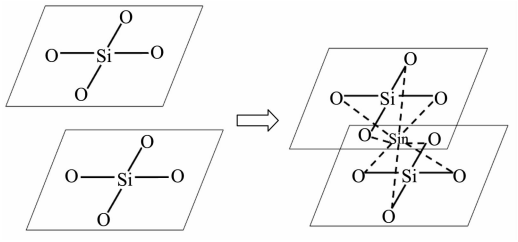

(a) SiO_2; (b) $n_{Sm^{3+}}/n_{SiO_2}$=15%

Fig.7 Frameworks of samples thermal treated at 700 ℃

2.4 Photoluminescence

The PL emissions with excitation at 380 nm for SiO_2:Sm are shown in Fig.8. The PL spectra cover a large part of the visible spectra, from 420 to 700 nm. We think that the PL curves are composed of three PL components, i.e. component blue (maximum smaller than 500 nm), component green(maximum smaller than

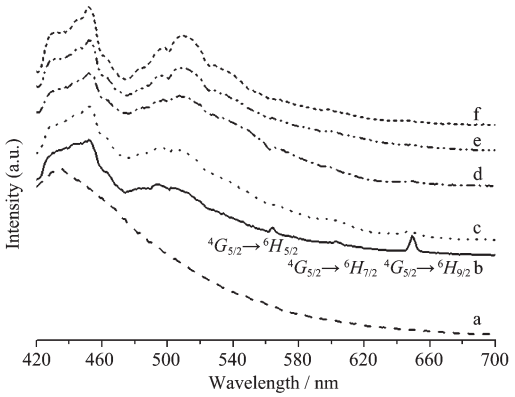

(a) SiO_2; (b) 2.5mol%; (c) 5mol%; (d) 10mol%; (e) 15mol%; (f) 20mol%

Fig.8 Photoluminescence spectra of samples with different doping concentrations of Sm^{3+} excitation at 380 nm

590 nm), and component red (maximum smaller than 700 nm) in allusion to the region where the maxima of component appears. SiO_2 sample only has an emission peak at 435 nm, compared to the samples doped with different concentrations of Sm^{3+} showing higher PL intensity near 450 nm and 500 nm. The blue-green light emission for the PL curves is enhanced with the increasing samarium content, while the red component of PL decreases at the same time.

The PL spectra at 560, 600 and 650 nm are the typical samarium emissions due to $^4G_{5/2}\rightarrow{}^6H_{5/2}$, $^4G_{5/2}\rightarrow{}^6H_{7/2}$ and $^4G_{5/2}\rightarrow{}^6H_{9/2}$ transitions in the visible region, respectively [28]. On the other hand, the PL process is associated with the specific structure of Si-O framework. The silicon tends ideally to bond with four oxygen atoms. However, by doping with samarium ion, the structure becomes a mixture of SiO_x clusters(x=3 or 4 mostly) intercalated with interstitials Sm. The increasing doping concentration of Sm^{3+} provokes an increase in the concentration of SiO_3-SiO_4 clusters, and yields higher PL intensity. So the powders have certain amount of disorder that gives the ideal condition to appear as the intense blue-green PL. Finally, it can be proposed that the PL intensity due to Sm^{3+} ion and the broad band can be used as a probe of the disorder gradient in the short- and long-range environments of Si.

The increasing doping concentration of Sm^{3+} causes more formation of Si-O-Sm linkages accompanied by

the creation of electron-captured oxygen vacancies, V_O, as $[SiO_3\text{-}V_O\text{-}SiO_4]$ complex. This means that most of the electrons around oxygen vacancies are released, and such oxygen vacancy sites are relatively positive charged. Consequently, the oxygen vacancies tend to trap photo-generated electrons. In the complex, the Si-O without introduction of samarium ion acts as hole traps, while the vacancy V_O tends to trap electrons. It is well known that electrons determine the transport properties like the electrical conductivity, while no phenomena related to holes have been observed. This indicates that holes are almost all trapped around defects. Therefore, Si-O-Sm linkage is the key factor to influence photoluminescence.

3 Conclusion

A composite material SiO_2:Sm was obtained by the sol-gel process. The FTIR peaks near 960 cm^{-1} are assigned to the deformation vibration of Si-O-Sm linkages. The samarium ion has been incorporated into the framework of SiO_2 to form Si-O-Sm linkages as evidenced by ^{29}Si MAS-NMR analysis. The introduction of samarium ion into the SiO_2 allows special blue-green and red PL emission of the SiO_2:Sm compound could be observed due to the formation of Si-O-Sm linkages accompanied by the creation of electron-captured oxygen vacancies.

References:

[1] Kenyon A J, Chryssou C E, Pitt C W, et al. *J. Appl. Phys*., **2002**,**91**(1):367~374

[2] Yan B, Huang H H. *Colloids Surf. A*, **2006**,**287**(1~3):158~162

[3] Yokoyama H. *Science*, **1992**,**256**(5053):66~70

[4] Richardson F S. *Chem. Rev*., **1982**,**82**(5):541~552

[5] Buonocore G E, Li H, Marciniaak B, et al. *Coord. Chem. Rev*., **1990**,**99**:55~87

[6] Jin T, Tsutsumi S, Deguchi Y, et al. *J. Electrochem. Soc*., **1995**,**142**(10):195~197

[7] Dong D W, Jiang S C, Men Y F, et al. *Adv. Mater.*, **2000**,**12**(9):646~649

[8] Binnemans K, Lenaerts P, Driesen K, et al. *J. Mater. Chem.*, **2004**,**14**:191~195

[9] Driesen K, Van D R, GÖrller-Walrand C, et al. *Chem. Mater.*, **2004**,**16**(8):1531~1535

[10] Lenaerts P, Storms A, Mullens J, et al. *Chem. Mater.*, **2005**,**17**(20):5194~5201

[11] Lima P P, Sá Ferreira R A, Freire R O, et al. *Chem. Phys. Chem*., **2006**,**7**(3):735~746

[12] Fernandes M, Bermudez V de Z, Sá Ferreira R A, et al. *Chem. Mater*., **2007**.**19**(16):3892~3901

[13] Molina C, Dahmouche K, Messadeq Y, et al. *J. Lumin*., **2003**, **104**(1~2):93~101

[14] Peng C Y, Zhang H J, Yu J B, et al. *J. Phys. Chem. B*, **2005**, **109**(32):15278~15287

[15] Guo X M, Wang X M, Zhang H J, et al. *Microporous Mesoporous Mater.*, **2008**,**116**(1~3):28~35

[16] Aquino J M F B, Araujo A S, Melo D M A, et al. *J. Alloys Compd.*, **2004**,**374**:101~104

[17] Ikeda M, Uchida S. *Phys. Stat. Sol*., **2002**,**194**(2):407~413

[18] Yan B, Zhou K. *J. Alloys Compd.*, **2005**,**398**(1~2):165~169

[19] Alberthmeiry T de F, Valéria M L, Sérgio de L, et al. *J. Lumin.*, **2007**,**126**(10):403~407

[20] Zhang W F, Yin Z, Zhang M S. *Appl. Phys. A*, **2000**,**70**(1):93~96

[21] Selvaraj M, Pandurangan A, Seshadri K S, et al. *Appl. Catal. A*, **2003**,**242**(2):347~364

[22] YIN Wei (尹 伟). *Chinese J. Lumin.* (*Faguang Xuebao*), **2005**,**26**(8):473~477

[23] QIU Jian-Bin(邱健斌), LIU Yun-Zhen(刘云珍), LI Zhong-Shui(李忠水), et al. *J. Chinese Rare Earth Soc.* (*Zhongguo Xitu Xuebao*), **2002**,**20**(Spec. Issue):19~20

[24] Ge X G, Shi L, Wei J X, et al. *J. Rare Earths*, **2007**,**25**(5):321~328

[25] Kamal M S K. *J. Colloid Interface Sci.*, **2007**,**315**(2):562~568

[26] Caponetti E, Minoja A, Saladino M L, et al. *Microporous Mesoporous Mater*., **2008**,**113**(1~3):490~498

[27] Zhuang J Q, Ma D, Yang G, et al. *J. Catal*., **2004**,**228**(1):234~242

[28] Tan W M, Lu C H, Zhang Y, et al. *J. Rare Earths*, **2007**,**25**(S1):334~337